DRAFT SF 298

1. Report Date (dd-mm-yy)	2. Report Type	3. Dates covered (from... to)

4. Title & subtitle	5a. Contract or Grant #
Evaluation of the Corrosion Behavior of Storage Container Alloys in Halon 1301 Replacement Candidate Agents Tri-Service Conference on Corrosion Proceedings	
	5b. Program Element #

6. Author(s)	5c. Project #
Dante , J. F. , Stoudt, M.. R., Fink, J. L., Beauchamp , C. R., Moffat, T. P., Ricker, R. E.	5d. Task #
	5e. Work Unit #

7. Performing Organization Name & Address	8. Performing Organization Report #

9. Sponsoring/Monitoring Agency Name & Address	10. Monitor Acronym
Tri-Service Committee on Corrosion USAF WRIGHT-PATTERSON Air Force Base, Ohio 45433	11. Monitor Report #

12. Distribution/Availability Statement
Approved for Public Release
Distribution Unlimited

13. Supplementary Notes

14. Abstract

DTIC QUALITY INSPECTED 3

15. Subject Terms
Tri-Service Conference on Corrosion

Security Classification of			19. Limitation of Abstract	20. # of Pages	21. Responsible Person (Name and Telephone #)
16. Report	17. Abstract	18. This Page			

TRI-SERVICE CONFERENCE ON CORROSION

1994 TRI-SERVICE · DEPARTMENT OF DEFENSE · UNITED STATES OF AMERICA · CONFERENCE ON CORROSION

21-23 JUNE 1994

**SHERATON PLAZA HOTEL
ORLANDO, FLORIDA**

PROCEEDINGS

Evaluation of the Corrosion Behavior of Storage Container Alloys in Halon 1301 Replacement Candidate Agents

*Mr. J. F. Dante
Mr. M. R. Stoudt
Mr. J. L. Fink
Mr. C. R. Beauchamp
Dr. T. P. Moffat
Dr. R. E. Ricker
Materials Science and Engineering Laboratory
National Institute of Standards and Technology
Gaithersburg, Md. 20899

Introduction

The Montreal Protocol of 1987 identified a number of halogenated chemicals which possess sufficient stratospheric ozone depletion potentials to warrant limitations on their production and use. Included on this list was Halon 1301 (CF_3Br), the fire suppression agent of choice for aircraft engine nacelles and dry bays (1). As a result, the relative performance of different chemical compounds with low ozone depletion potentials were evaluated as a CF_3Br fire suppressant replacement. Since corrosion of fire suppressant containers by the agent could affect the reliability of these vessels, the corrosion behavior of typical alloys used in these containers needed to be evaluated. Mass change tests were performed for 1 month in different agents at 150 °C. Electrochemical tests were desired to supplement and possibly replace the current mass change experiments. A major advantage of electrochemical testing is the significant reduction in time required to estimate corrosion rates and the effect that pollutants (HF, HCl, and H_2O) in various agents, compositional changes, and the temperature have on the corrosion rate.

The goal of this study is to 1) determine which alternative fire suppressants are most compatible with the metals used in storage vessels and 2) to determine which storage container metals have the highest corrosion resistance when exposed to alternative fire suppressants. Since no test methodology existed at the start of this phase of the work, mass change tests were used to evaluate the field of possible fire suppressant agents and container alloys in terms of corrosivity and corrosion resistance, respectively. Simultaneously, an electrochemical test was developed in order to perform accelerated testing of the corrosion resistance of storage container alloys in halon fire suppression alternatives.

* presenting author

/

Experimental Details

Mass change exposures

Experiments were designed and conducted to evaluate the corrosivity of the different potential fire suppressants during normal service in aircraft storage containers. These experiments had to consist of exposures that emulate the conditions under which corrosion is expected to occur followed by careful examination and evaluation of the resulting corrosion damage. Smooth coupon exposure tests, were conducted to evaluate changes in mass during exposure thereby yielding a measurement of the rate of formation of corrosion scales or removal of metallic species. The coupons were examined visually and by optical microscopy to assess the occurrence of pitting, intergranular corrosion and dealloying. From the mass change and the exposure time, the average mass change rate can be estimated allowing comparison between the agents and alloys. Tests to study localized corrosion and environmentally induced fracture were also conducted and the results are described elsewhere (2).

The materials chosen for this study were: 304 stainless steel, 13-8 Mo stainless steel, AM 355 stainless steel, stainless steel alloy 21-6-9 (Nitronic 40), 4130 alloy steel, Inconel alloy 625, CDA-172 copper/beryllium alloy and 6061-T6 aluminum alloy. The compositions of these alloys are given in Table 1. These alloys were selected for these experiments based on discussions with the Air Force on the materials typically used for aircraft storage container components.

The samples used for the mass change experiments were flat smooth surface coupons; width = 25.4 mm, length = 50.8 mm, and thickness = 1.6 mm. A 6.7 mm diameter hole was drilled in the center of the coupons. After machining, the surfaces were glass bead blasted to remove any remaining surface oxides or scale and to provide a consistent smooth surface finish (120 grit nominal). Each sample was then ultrasonically cleaned, first in acetone and then in alcohol, dried with warm air and immediately weighed. Three separate weighings were taken at approximately 30 second intervals and averaged. This average value was then referred to as the initial weight of the coupon. The balance used for these weight measurements was self calibrating on start-up to maintain an accuracy to within $\pm 10 \times 10^{-6}$ g with a reproducibility of no less than $\pm 1.51 \times 10^{-8}$ g. Representative photographs of the surface of each alloy were also taken prior to the start of testing.

At the start of each exposure test, three coupons of each of the eight alloys were mounted on a polytetrafluoroethylene (PTFE) rod with PTFE spacers between the samples as shown in Figure 1a. This was done to separate and electrically isolate the samples thereby eliminating the possibility of galvanic coupling. Three samples of each type of alloy were used and PTFE shields were placed between the different types of alloys to protect the samples from contact with any corrosion products that may form. The samples were next placed in a PTFE lined, two liter pressure vessel for testing. The vessel was then attached to a mechanical vacuum pump and evacuated for a minimum of 30 minutes.

2

Table 1
The Composition of the alloys listed in weight percent.

| Element	Nit 40	Al 6061-T6	In 625	304 SS	CDA 172	13-8 Steel	SS Am355	AISI 4130
Ni	7.1	- -	61.39	8.26	0.06	8.4	423	0.08
Cr	19.75	0.04	21.71	18.11	0.01	12.65	15.28	0.98
Mn	9.4	0.15	0.08	1.41	- -	0.02	0.8	0.51
Mg	- -	1	- -	- -	- -	- -	- -	- -
Si	0.5	0.4	0.09	0.49	0.08	0.04	0.16	0.23
Mo	- -	- -	8.82	0.17	- -	2.18	2.6	0.16
N b	- -	- -	3.41	- -	- -	- -	- -	- -
N	0.29	- -	- -	0.03	- -	0	0.12	- -
C	0.02	- -	0.02	0.06	- -	0.03	0.12	0.32
B e	- -	- -	- -	- -	1.9	- -	- -	- -
Co	- -	- -	- -	0.11	0.2	- -	- -	- -
Zn	- -	0.25	- -	- -	- -	- -	- -	- -
Cu	- -	0.15	- -	- -	97.9	- -	- -	- -
Fe	bal	0.7	3.97	bal	0.06	bal	bal	bal
Al	- -	bal	0.23	- -	0.04	1.11	- -	0.04
G/cm^3*	7.83	2.7	8.44	7.94	8.23	7.76	7.91	7.85

* Nominal Density

The mass of agent required to produce a pressure of approximately 5.86 MPa at 150 °C was determined from a computer program based on the available thermodynamic data, and the gas laws. To facilitate charging of the agents, the test vessels were chilled in a bath of either ice and water, or dry ice and alcohol, depending on the temperature necessary to maintain the liquid phase. The vessels were then placed on a balance that allowed weighing of the entire vessel and determination of the mass of the agent added continuously during filling. Upon completion of the charging step, the vessels were placed in proportionally controlled, calrod-type heaters that kept the temperature constant at 150 ±1 °C for the 25 day exposure period.

At the conclusion of the testing period, the heaters were turned off and the vessels were allowed to cool naturally to ambient temperature. After the agent was released, the coupons were extracted and immediately reweighed using the same procedure that was used for the initial weight measurements. The average of those three measurements was then referred to as the final weight of the coupon. Representative photographs of the surfaces were again taken and compared to those of the initial condition.

Electrochemical Measurements
Electrochemical testing offers the possibility of more rapid evaluation of the corrosion rate and the effect of contaminants, material composition and temperature. Furthermore, numerous analytical electrochemical methods may be used to investigate the mechanisms of corrosion (3). However, the high resistivity of the aliphatic hydrocarbon solvents makes the implementation of such measurements extremely difficult, e.g. Halon 124, CF_3CHClF has a

General Corrosion Samples

PTFE Gasket

Teflon devider

Teflon spacer

Teflon insert
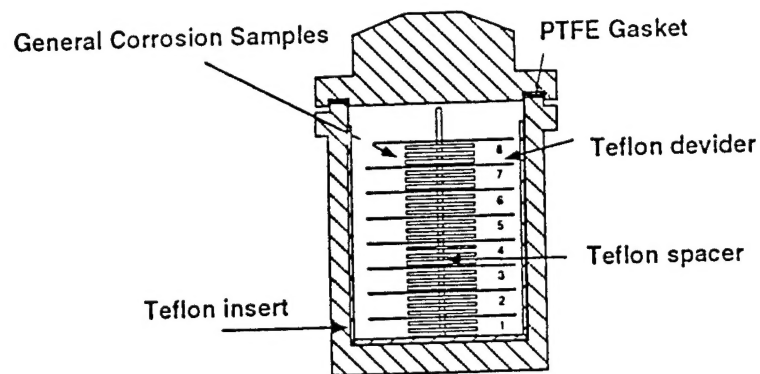
1 = Al Alloy AA 6061-T6	5 = In 625
2 = Cu Alloy CDA-172	6 = 304 Stainless Steel
3 = AM 355	7 = AISI 4130 Steel
4 = 13-8 Mo Steel	8 = Nitronic 40

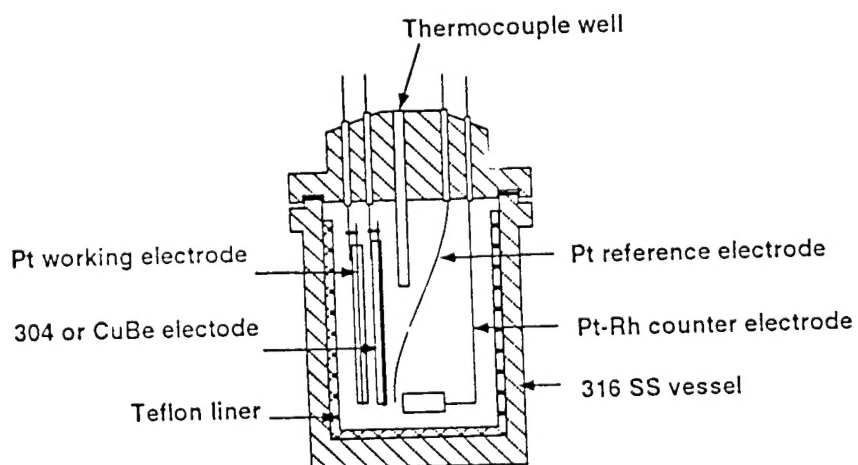Fig. 1a: Immersion testing chamber for smooth coupon weight loss measurements.

Thermocouple well

Pt working electrode

Pt reference electrode

304 or CuBe electode

Pt-Rh counter electrode

316 SS vessel

Teflon liner

Fig. 1b: Electrochemical cell.

4

resistivity of $\sim 1.5 \times 10^9$ ohm • cm. This value is similar to that observed for other non-aqueous solvents, i.e. acetonitrile, CH_3CN (4). In order to perform electrochemical measurements in such media a supporting electrolyte is required (4). Unfortunately, simple inorganic salts like NaCl or Na_2SO_4 are essentially insoluble in aliphatic solvents due to the low dielectric constant of the solvent, i.e. CF_3CHClF, $\varepsilon \sim 6.73$. However, quaternary ammonium salts are known to be soluble in low dielectric constant media such as dichloromethane and chloroform, $\varepsilon = 8.93$ and 4.81 respectively (5). Thus, we have investigated tetrabutylammonium hexafluorophosphate (Bu_4NPF_6) as a potential supporting electrolyte. In order to demonstrate the ability to perform well defined electrochemical measurements in the halon alternatives, the electrochemistry of a simple outer-sphere redox couple, ferrocene/ferrocenium ($Cp_2Fe^{0/+}$) was investigated by cyclic voltammetry (CV) at a platinum electrode. Because of its nonpolar character, ferrocene readily dissolves in aliphatic hydrocarbons like CF_3CHClF. This redox couple was also used to establish a reference potential (5).

A multipurpose high-pressure cell was designed for making electrochemical measurements in the halon alternative environments (manufactured by PARR Moline, Ill.). The vessel is made of 0.635 cm thick 316 stainless steel and is rated to ~ 6.9 MPa of pressure. The head of the cell was outfitted with four electrical feed throughs for performing two, three or four electrode electrochemical experiments. The vapor pressure in the cell was monitored by a pressure gauge mounted on the head of the cell. At higher temperatures, most of the alternative fire suppressants reach very high vapor pressures so a pressure release valve is incorporated in case of accidental over pressurization. Temperature was monitored with a thermocouple mounted in a well in the cell top. A teflon insert was used to prevent accidental electrical contact between the electrodes and the stainless steel cell. The insert also helped to minimize interactions between the electrolyte and the 316 cell wall. A schematic of the three electrode cell configuration is shown in Fig 1b. Measurements were made using an EG&G PAR 273 potentiostat / galvanostat in potentiostatic mode and M270 software.

All of the electrochemical tests were conducted in HCFC 124, CF_3CHClF, which has a vapor pressure of 3.393×10^5 Pa at 20 °C. The conductivity was increased by adding 5×10^{-2} moles/ liter Bu_4NPF_6 (Aldrich). The cell top was left slightly opened and argon was flowed into the cell in order to remove water vapor. The head of the cell was then bolted down and the entire cell was chilled in dry ice. Chilling helped expedite filling of the cell with agent. After chilling, approximately 352 grams of CF_3CHClF were transferred into the cell. This resulted in about 3 cm, or 250 ml, of CF_3CHClF in the liquid phase in the bottom of the cell at room temperature. A large platinum rhodium electrode was used as a counter electrode and a separate platinum wire was used as a quasi-reference electrode. The quasi-reference electrode was placed between the counter and the working electrode. Heat shrinkable teflon tape was used to connect the electrodes to the electrical feed throughs and clips were used to make electrical contact.

In the first experiments 0, 5×10^{-4}, or 1×10^{-3} moles/ liter ferrocene (98% Aldrich) was added to the electrolyte. The tests were run at room temperature, 20 °C. A platinum disk working electrode (area = 0.00317 cm^2) was prepared by encapsulating a platinum wire in glass followed by polishing to a 1μm finish. The potential scale of each experiment was referenced to a platinum quasi-reference electrode and then normalized afterwards to the half-wave potential of $Cp_2Fe^{0/+}$.

In subsequent experiments the slow sweep rate voltammetric or potentiodynamic characteristics of 304 stainless steel (area = 0.00785 cm^2)(Goodfellow) and Cu-1.9 wt%Be (area = 0.00196 cm^2)(Goodfellow) were investigated in 5×10^{-2} moles/ liter Bu_4NPF_6 in CF_3CHClF. These electrodes were encapsulated in glass and polished to a 1 μm finish. Voltammetry of a platinum electrode in the same electrolyte helped establish the potential scale as revealed by the potential at which reduction of the electrolyte occurs. The potential axis of the voltammograms was then referenced to the half-wave potential of $Cp_2Fe^{0/+}$.

Results and Discussion
Mass change exposures
The mean mass changes observed from three samples of each of the alloys on exposure to each of the agents for 25 days at 150 °C are given in Table 2 and the standard deviations determined for these measurements are given in Table 3. All of the mass changes are relatively small and most represent an increase in mass (positive values in Table 2). The mass change rate was estimated from these measurements by the relationship

$$R= \Delta M/(At) \tag{1}$$

where ΔM is the mass change, A is the total exposed area of the sample and t is the exposure time in days. This relationship estimates the average mass change rate over the exposure period and assumes that the mass change rate was essentially constant over the entire exposure period.

Table 4a gives a numerical value to an absolute mass change rate range as well as the equivalent penetration rate for each alloy for mass loss at the maximum rate for the range. The absolute value of the mass change rate, from Equation 1 and Table 2, for each alloy was compared with Table 4a and assigned a numerical rating, Table 4b. It was assumed that a mass increase was due to the formation of a surface film which formed as a result of exposure to residual gases, decomposition gases, or the agents themselves. In any case, the film composition will contain either a fraction of or no metal. Also, the corrosion rate for a metal with a surface film tends to decrease with time. Thus, the calculated rate of mass increase, and hence the numerical rating, will be an overestimate of the corrosion damage.

Taking into account propagation errors in both area and time measurements (6), it can be shown, in some instances, that the maximum and minimum confidence levels of the mass change rate, at 90% confidence,

6

Table 2
Mean Mass Change for Each Alloy in Each Agent
After 25 Day Immersion at 150°C [mg]

Positive Values = Scaling
Negative Values = Mass Loss

Environ-ment	Nit 40	Al 6061	In 625	304 SS	CDA 172	13-8 Steel	AM 355	AISI 4130	Agent Avg.	Std. Dev.
HCFC-22	0.176	0.458	-0.329	0.168	3.064	-0.033	-0.087	2.847	0.783	1.362
HCFC-124	0.092	0.219	-0.267	-0.037	1.474	-0.086	-0.206	0.319	0.189	0.557
FC-31-10	0.247	0.533	-0.037	0.583	2.663	0.357	0.219	1.102	0.708	0.858
HFC-227	0.009	0.128	-0.056	0.141	1.973	0.069	0.007	0.297	0.321	0.676
HFC-125	-0.011	0.199	0.031	0.136	0.89	0.151	0.029	0.673	0.262	0.333
FC-116	0.006	0.24	0.026	0.147	1.509	0.21	0.139	0.403	0.335	0.491
HFC-134a	0.013	0.131	-0.103	0.069	0.229	0.088	-0.014	0.262	0.084	0.122
HFC-236	0.024	2.479	-0.063	0.078	0.866	0.107	0.007	0.343	0.48	0.861
FC-C318	0.008	1.183	0.018	0.199	0.431	0.169	0.006	0.31	0.29	0.392
FC-218	0.153	0.373	0.051	0.09	0.768	0.279	0.15	0.381	0.281	0.232
HFC-32/125	0.3	0.587	0.146	0.241	2.263	0.492	0.211	0.227	1.96	3.851
NaHCO3	0.396	1.038	0.079	0.262	2.182	0.8	0.259	0.89	0.738	0.677
Alloy Avg.	0.118	0.631	-0.042	0.173	1.526	0.217	0.068	1.597		
Std. Dev.	0.137	0.675	0.138	0.152	0.911	0.243	0.15	3.152		

Table 3
Standard Deviation of mass change measurements
for each alloy in each environment (mg).

Environ-ment	Nit 40	Al 6061	In 625	304 SS	CDA 172	13-8 Steel	AM 355	AISI 4130	Agent Avg.
HCFC-22	0.079	0.113	0.088	0.057	0.331	0.043	0.05	1.28	0.255
HCFC-124	0.045	0.091	0.048	0.04	0.294	0.072	0.103	0.099	0.099
FC-31-10	0.04	0.079	0.028	0.035	0.107	0.07	0.046	0.173	0.072
HFC-227	0.034	0.043	0.018	0.025	0.159	0.063	0.02	0.047	0.051
HFC-125	0.121	0.117	0.044	0.013	0.018	0.014	0.007	0.091	0.053
FC-116	0.124	0.087	0.025	0.033	0.157	0.012	0.063	0.013	0.064
HFC-134a	0.021	0.025	0.024	0.002	0.039	0.061	0.048	0.091	0.039
HFC-236	0.024	1.895	0.03	0.03	0.028	0.015	0.09	0.043	0.269
FC-C318	0.04	0.602	0.065	0.054	0.072	0.014	0.109	0.035	0.124
FC-218	0.083	0.048	0.011	0.05	0.032	0.021	0.044	0.08	0.046
HFC-32/125	0.033	0.324	0.022	0.037	0.217	0.14	0.035	0.122	0.116
NaHCO3	0.297	0.501	0.022	0.047	0.235	0.263	0.042	0.168	0.197
Alloy Avg.	0.078	0.327	0.035	0.035	0.141	0.066	0.055	0.187	

Table 4a
Mass Change Rate Values used in rating alloy/agent behavior and equivalent penetration rate based on alloy nominal density

based on absolute value of mass change rate
penetration valid only for mass loss

Score	Mass Chg Rate mg/(m^2-d) Lower Bound	Upper Bound	Equivalent Penetration Rate for Upper Boundary μm/year							
			Nit 40	Al 6061	In 625	304 SS	CDA 172	13-8 Steel	AM 355	AISI 4130
1	0	0.1487	0.0069	0.0201	0.0064	0.0068	0.0066	0.007	0.0069	0.0069
2	0.1487	0.923	0.0431	0.1249	0.0399	0.0425	0.041	0.0434	0.0426	0.0429
3	0.923	5	0.2332	0.6764	0.2164	0.23	0.2219	0.2353	0.2309	0.2326
4	5	25	1.166	3.382	1.082	1.15	1.109	1.177	1.154	1.163
5	25	125	5.831	16.909	5.409	5.75	5.547	5.883	5.772	5.816
6	125	600	27.99	81.16	25.96	27.6	26.63	28.24	27.7	27.92
7	600	3,000	139.9	405.8	129.8	138	133.1	141.2	138.5	139.6
8	3,000	15,000	699.7	2029.1	649.1	690	665.7	706	692.6	697.9
9	15,000	75,000	3498	10146	3246	3450	3328	3530	8463	3490
10	75,000	--	--	--	--	--	--	--	--	--

Table 4b
Mass Loss Rate Evaluation of Agents and Alloys based on 25 day immersion at 150 C

Environment	Nit 40	Al 6061	In 625	304 SS	CDA 172	13-8 Steel	AM 355	AISI 4130	Agent Avg.	Std. Dev.	Agent Rank
HCFC-22	3	4	3	3	5	2	3	5	3.5	1.07	9
HCFC-124	3	3	3	2	4	3	3	3	3	0.53	7
FC-31-10	3	4	2	4	5	4	3	4	3.63	0.92	11
HFC-227	1	3	2	3	5	3	1	3	2.63	1.3	1
HFC-125	2	3	2	3	4	3	2	4	2.88	0.83	4
FC-116	1	3	2	3	4	3	3	4	2.88	0.99	4
HFC-134a	2	3	3	3	3	3	2	3	2.75	0.46	3
HFC-236	2	5	2	3	4	3	1	3	2.88	1.25	4
FC-C318	1	4	2	3	4	3	1	3	2.63	1.19	1
FC-218	3	4	2	3	4	3	3	4	3.25	.1	8
HFC-32/125	3	4	3	3	5	4	3	3	3.5	0.76	9
NaHCO3	4	·	3	3	5	4	3	4	3.75	0.71	12
Alloy Avg.	2.33	3.67	2.42	3	4.33	3.17	2.33	3.58			
Std. Dev.	0.98	0.65	0.51	0.43	0.65	0.58	0.89	0.67			
Alloy Rank	1	7	3	4	8	5	1	6			

Score	Freq.	
1	6	No evidence of attack (t<0.741, 50% CI).
2	14	Some inconclusive evidence of attack (0.741(50% CI) < t < 4.6 (99% CI)).
3	47	Conclusive evidence of attack (t>4.6, 99% CI).
4	22	Corrosion of little concern, (less than =1 μm/year, 3μm for Al alloy).
5	7	Corrosion may be a concern
6	0	Corrosion rate should be considered in design
7	0	Corrosion about 1 to 5 mils per year
8	0	Rapid Corrosion
9	0	V~ry rapid corrosion
10	0	Extremely rapid corrosion

spans zero. This would indicate that we can not conclude that the corrosion rate is a value other than zero. However, a film appeared on the surfaces of many of these samples and there was evidence of spalling. These films were very thin and could be detected by a color change in the samples. Thus, it is believed that the confidence interval spans zero as a result of scaling of the metal surface followed by the spalling of this scale which increased the measurement scatter.

Mass increases are not uncommon during immersion testing and usually descaling techniques are employed to remove these scales for the determination of the remaining metal. Considerable research has been conducted in the area of descaling. Despite this concerted effort, however, some metal is removed in the descaling process. For long exposures or thick films. the metal is only a small fraction of the material removed and errors are small. In this study, the films are very thin and removal of any metal by descaling would result in significant errors. Additionally, techniques for descaling metals that were exposed to organic environments are not well developed. For these reasons, descaling was not attempted in this investigation.

Evaluation of the relative performance of the alloy/ agent combinations was hampered by the comparison of mass loss and mass gain measurements. Typically, mass loss measurements are evaluated by assuming that all of the lost mass was the result of corrosion and that no corrosion products were left on the surface to create errors in this determination. Then, the quantity of metal reacting and rate of the reactions can be calculated directly from the mass loss. Similarly, mass gain measurements can be evaluated if the reaction and the reaction products are known and it is assumed that none of the scale spalls off and is lost to the environment. However, when these are not known, evaluation contains greater uncertainties, but it is clear that the relative magnitude of mass change is still related to the reaction rate between the metallic species and the environment.

According to Table 4b, the most suitable materials for use in storage containers are Nit 40, SS AM355, In 625, and 304 SS. The most suitable agents for use as alternative fire suppressants from a corrosion viewpoint are HFC-227, FC-C318, HFC-134a, HFC-125, FC-166, and HFC-236. This ranking of materials and agents is based solely on smooth coupon exposure tests, however, and may change when other corrosion tests are taken into consideration (1).

Electrochemistry
Cyclic voltammetry of $Cp_2Fe^{0/+}$

A cyclic voltammogram for a Pt electrode in a solution containing 5 x 10^{-2} moles/ liter Bu_4NPF_6 reveals the onset of oxidation of the system at 1.2 V (vs PtQRE) and the reduction of electrolyte begins at -0.96 V (vs. PtQRE). The magnitude of the wave at -0.96 V varies each time the cell is reassembled and is thought to be the result of water contamination. This is
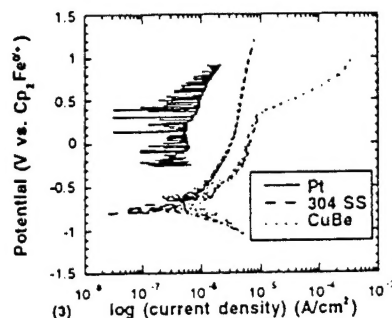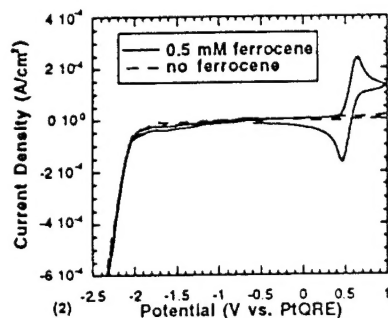
Fig. 2: 0.1 V/ s CV scan of ferrocene on a Pt electrode in CF_3CHClF with 5 x 10^{-2} moles/ liter Bu_4NpF_6.

Fig. 3: 1 mV/ s anodic polarization scan of Pt, 304 SS, and CuBe in CF_3HClF with 5 x 10^{-2} moles/ liter Bu_4NPF_6.

supported by other experiments which demonstrated that the magnitude of the reduction wave scaled with the level of controlled H_2O doping of the electrolyte. Nonetheless, another reduction process becomes apparent at ~ -1.79 V (vs. PtQRE) and increases rapidly below ~ - 2.02 V (vs. PtQRE). This latter value is similar to that observed for reduction of Bu_4N^+ in CH_3CN although reduction of the solvent may also occur in this potential regime (4). The position of the background reduction process remained unchanged throughout each series of tests, indicating there was no potential drift during the tests. Thus, the electrolyte exhibits at least a 2.16 V window where no reactions occur on platinum.

Performing the same experiment with 5 x 10^{-4} moles/ liter ferrocene added to electrolyte reveals a well defined quasi-reversible redox wave due to ferrocene oxidation and ferrocenium reduction as shown in Fig. 2. For a sweep rate of 0.1 V/s the peak potential spitting is 0.18 V. A reversible process should exhibit a value of 0.06 V. This deviation from reversibility may be due to slow electron transfer kinetics, or alternatively, may be an artifact of uncompensated solution resistance. For example, at sweep rates above 2 V/s the shape of the voltammogram is severely distorted due to iR effects. Nonetheless the peak current at slower sweep rates may be used to estimate the diffusion coefficient of ferrocene (3, 5) by assuming that the wave is reversible. The Randles-Sevcik equation (3) yields a diffusion coefficient of 3.26 x 10^{-5} cm^2/s. The anodic and cathodic peaks of $Cp_2Fe^{0/+}$ are centered at 0.56 V (vs PtQRE). In another experiment, a doubling of the ferrocene concentration to 1 x 10^{-3} moles/ liter resulted in a doubling of the peak oxidation current. These experiments demonstrate the ability to

perform quantifiable electrochemical experiments in halon alternative solvents.

$Cp_2Fe^{0/+}$ Reference Electrode

The well defined nature of the $Cp_2Fe^{0/+}$ reaction may be used to firmly establish the potential scale. The platinum quasi reference scale while useful as a working reference, does not have a clear meaning in terms of a chemical potential. However, by noting the difference, -2.58 V between the onset of electrolyte reduction on a platinum working electrode at -2.02 V (vs PtQRE) and the half wave potential for $Cp_2Fe^{0/+}$ 0.56 V (vs PtQRE) in the same solution, we can calibrate the potential scale of similar experiments performed in a ferrocene-free electrolyte by measuring the potential at which the onset of electrolyte breakdown occurs on platinum (vs a quasi reference electrode) and set the numerical value to -2.58 V vs $Cp_2Fe^{0/+}$. Thus, in the remaining portion of this manuscript the potential scale is referenced to $E_{1/2}(Cp_2Fe^{0/+}) = 0.0$ V.

Potentiodynamic curves for Cu-1.9wt%Be and 304 SS

The i-E characteristics of Pt, Cu-1.9wt%Be and 304 SS are shown in Figure 3. A small anodic background current was observed on Pt probably associated with the oxidation of impurities in the electrolyte. The 304 SS exhibits polarization characteristics of a spontaneously passive alloy with a near potential independent passive current in the range of 1-10 $\mu A/cm^2$. In contrast Cu-1.9wt%Be exhibits a rapid increase in the dissolution rate at 0.4 V. Analysis of the electrode after removal from the cell revealed substantial metal loss. It is important to recall that the long term high temperature mass change experiments revealed a measurable mass change from the Cu-1.9wt%Be alloy while negligible attack was found for 304 SS. The favorable qualitative agreement between the mass change and electrochemical measurements clearly indicates that we can differentiate the susceptibility of various alloys to corrosion in fire suppressant media via rapid electrochemical experimentation. Future work will attempt to determine the affect of temperature, pollutant gasses, and water contamination on the corrosivity of metals in halon alternative media.

Conclusions

A program is underway to find an alternative fire suppressant to halon 1301. The selection of a replacement agent is, at least in part, dependant upon the corrosivity of the replacement agents towards storage container materials. Mass change data for flat smooth coupons of several such materials in replacement candidates has been presented. A ranking of the agents and container materials was evaluated based on this data. It was found that Nit 40, AM355, In 625, and 304 SS suffered the least amount corrosion damage. Agents that caused, on average, the least amount of corrosion damage were HFC-227, FC-C318, HFC-134a, HFC-125, FC-116, and HFC-236. It should be noticed, however, that a complete evaluation of the corrosion performance of the agent / alloy system would

include tests for localized corrosion and environmentally induced fracture.

An electrochemical test is being developed as a supplement or possible alternative to the mass change tests. It has been shown that electrochemical measurements can be made in low conductivity halon alternative environments and that it is possible to rank materials based on their corrosion current densities.

References
1. R. G. Gann, et al., "Agent/System Compatibility for Halon 1301 Aviation Replacement - Comprehensive Test Plan", NIST TN 1278, NIST, (1992).

2. R. E. Ricker, M. R. Stos dt, J. F. Dante, J. L. Fink, C. R. Beauchamp, and T. P. Moffat in "Evaluation of Alternative In-Flight Fire Suppressants for Full-Scale Testing in Simulated Aircraft Engine Nacelles and Dry Bays", W. L. Grosshandler, R. G. Gann, and W. M. Pitts eds., NIST SP 861, U. S. Government Printing Office, Washington D. C., (1994).

3. A.J. Bard and L.R. Faulkner, "Electrochemical Methods, Fundamentals and Applications", John Wiley & Sons, Inc, N.Y., (1980).

4. D.T. Sawyer and J.L. Roberts, "Experimental Electrochemistry for Chemists", John Wiley & Sons, N.Y., (1974); P.T. Kissinger and W.R. Heineman, Laboratory Techniques in Electroanalytical Chemistry, Marcel Dekker, Inc, N.Y., (1984).

5. M.H. Pournaghi-Azar and R. Ojani, Electrochimica Acta, 39, ^53 (1994).

6. P. . .. Bevington, "Data Reduction and Error Analysis for the Physical Sciences". McGraw-Hill, New York, (1969).